Novel direct Method on the Life Prediction of Component under High Temperature–Creep Fatigue Conditions

Haofeng Chen[1,*], Yevgen Gorash[1]

[1] Department of Mechanical and Aerospace Engineering, University of Strathclyde, Glasgow G1 1XJ, UK
* Corresponding author: Haofeng.chen@strath.ac.uk

Abstract This paper presents a novel direct method, within the Linear Matching Method (LMM) framework, for the direct evaluation of steady state cyclic behaviour of structures subjected to high temperature – creep fatigue conditions. The LMM was originally developed for the evaluation of shakedown and ratchet limits. The latest extension of the LMM makes it capable of predicting the steady state stress strain solutions of component subjected to cyclic thermal and mechanical loads with creep effects. The proposed iterative method directly calculates the creep stress and cyclically enhanced creep strain during the dwell period for the assessment of the creep damage, and also creep enhanced total strain range for the assessment of fatigue damage of each load cycle. To demonstrate the efficiency and applicability of the method to assess the creep fatigue damage, two types of weldments subjected to reverse bending moment at elevated temperature of 550C are simulated by the proposed method considering a Ramberg-Osgood model for plastic strains under saturated cyclic conditions and a power-law model in "time hardening" form for creep strains during the dwell period. Further experimental validation shows that the proposed direct method provides a general purpose technique for the creep fatigue damage assessment with creep fatigue interaction.

Keywords Creep, Fatigue, Cyclically enhanced creep, Linear Matching Method, Weldment

1. Introduction

Engineering structures and components subjected to cyclic loading at elevated temperature means that the operating lifetime may be limited either by excessive plastic deformation, creep rupture, ratchetting, or cyclically enhanced creep deformation and total strain range enhanced by the creep-fatigue interaction. In order to assess the component lifetime associated with cyclic responses with creep fatigue interaction, construction of the hysteresis cycle (Fig. 1) is key to an R5 V2/3 assessment procedure [1] since it provides the strain range from which the fatigue damage is calculated, and the start-of-dwell stress σ_1 and creep strain ε^{cr}, from which the creep damage is assessed.

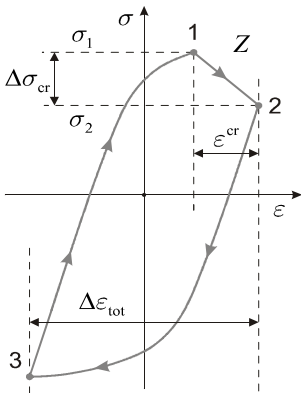

Figure 1. Typical saturated hysteresis loop with creep fatigue interaction

When a structural component is subjected to the cyclic load condition beyond the elastic shakedown limit, the introducing plastic strains will lead to the structure failure by either low cycle fatigue due to alternating plasticity or incremental plastic collapse due to ratchetting. In the presence of creep,

the response of the structure to cyclic loading changes significantly, due to the synergistic interaction of plasticity and creep. A structure subjected to cyclic loading with creep dwell period can present different asymptotic behaviours [2]: 1) no stress relaxation is taking place, as the accumulation of creep strain is determined by the steady-state primary load; 2) with a cyclically enhanced creep during dwell time, the stress relaxation process introduces an additional residual stresses field to enhance the total strain range, causing more significant creep and fatigue damages. In the asymptotic behaviour 2), a closed hysteresis loop could be generated if the creep dwell period is limited and the introducing creep strain could be recovered by the plastic strain during the unloading process.

In order to predict lifetime of component under high temperature and creep fatigue conditions, an evaluation of steady state cyclic behaviour of structures under such conditions would be necessary to construct a hysteresis loop. The simplified methods in R5 [1] assessment procedure for the high temperature response of structures are less restrictive than those based on elastic solutions, without requiring the complexity of full inelastic computation. These simplified approaches use reference stress and shakedown concepts and inevitably incorporate conservatism. Another method is to perform incremental step-by-step Finite Element Analysis (FEA). However, to achieving the steady state response of structures subject to cyclic loading, it requires a significantly large number of increments in full step-by-step analysis which becomes computationally expensive. Therefore, direct methods have been developed to assess the stabilised response of structures subject to cyclic loading. The Direct Cyclic Analysis (DCA) [3] has been recently incorporated into Abaqus [4] to evaluate the stabilized cyclic behaviour directly. This method uses a combination of Fourier series and time integration of the nonlinear material behaviour to obtain the stabilized cyclic response of the structure iteratively. Due to the characteristic of DCA and the inevitable numerical error due to the approximation and convergence problem, the DCA may not always be able to provide accurate solutions for complicated engineering problems.

In this paper, a novel direct method, the Linear Matching Method (LMM) [5, 6], is adopted for the direct evaluation of steady state cyclic behaviour of structures subjected to high temperature – creep fatigue conditions. The basis of the LMM is through the simple idea of representing histories of stress and inelastic strain as the solution of a linear problem where the linear moduli are allowed to vary both spatially and in time. In this way, the LMM combines both the convenience and efficiency of rule based methods [1] and the accuracy of simulation techniques. The LMM has been implemented into ABAQUS for all stages of life assessment code R5 [1] for the evaluation of high temperature responses of structures, based upon the same fundamental assumptions and materials database as R5 but with significantly greater accuracy. Typical of cyclic problems considered includes shakedown and limit analysis [7], ratchet limit analysis [8], creep rupture analysis [9], creep and fatigue interaction [5, 6]. The LMM ABAQUS user subroutines have been consolidated by the R5 research programme [10] of EDF energy to the commercial standard, and are counted to be the method most amenable to practical engineering applications involving complicated thermomechanical load history.

In this paper, the latest extension of the LMM [6] is summarised for directly predicting the steady state cyclic behaviour of component subjected to cyclic thermal and mechanical loads with creep effects. The efficiency and effectiveness of the method was validated in [6] through benchmark examples of Bree problem and a holed plate. In this paper, the developed method is further applied to more practical engineering applications, where two types of weldments subjected to different reverse bending moments with various creep dwell periods are simulated by the proposed method considering a Ramberg-Osgood model for plastic strains under saturated cyclic conditions and a power-law model in “time hardening” form for creep strains during the dwell period. The obtained

steady state cyclic stress strain solutions are then used to calculate the number of cycles to failure due to the creep fatigue damage, where the numerical lifetime results are validated by the existing experimental solutions [11, 12] for the Type 2 cruciform weldment.

2. Numerical Procedures

2.1. Asymptotic cyclic solution

We consider a structure subjected to a cyclic history of varying temperature $\lambda_\theta\theta(x_k,t)$ within the volume of the structure and varying surface loads $\lambda_p P(x_k,t)$ acting over part of the structure's surface S_T. The variation is considered over a typical cycle $0 \le t \le \Delta t$ in a cyclic state. Here λ_θ and λ_p denote the load parameters, allowing a whole class of loading histories to be considered. On the remainder of the surface S, denoted by S_u, the displacement u_k=0.

Corresponding to these loading histories there exists a linear elastic stress history:

$$\hat{\sigma}^e_{ij}(x_k,t) = \lambda_\theta \hat{\sigma}^\theta_{ij}(x_k,t) + \lambda_p \hat{\sigma}^p_{ij}(x_k,t) \tag{1}$$

where $\hat{\sigma}^\theta_{ij}$ and $\hat{\sigma}^p_{ij}$ denotes the varying elastic stresses due to $\theta(x_k,t)$ and $P(x_k,t)$, respectively. The asymptotic cyclic solution may be expressed in terms of three components, the elastic solution, a transient solution accumulated up to the beginning of the cycle and a residual solution that represents the remaining changes within the cycle. The general form of the stress solution for the cyclic problems involving changing and constant residual stress fields is given by

$$\sigma_{ij}(x_k,t) = \hat{\sigma}^e_{ij}(x_k,t) + \bar{\rho}_{ij}(x_i) + \rho^r_{ij}(x_k,t) \tag{2}$$

where $\bar{\rho}_{ij}$ denotes a constant residual stress field in equilibrium with zero surface traction on S_T and corresponds to the residual state of stress at the beginning and end of the cycle. The history ρ^r_{ij} is the change in the residual stress during the cycle and satisfies:

$$\rho^r_{ij}(x_k,0) = \rho^r_{ij}(x_k,\Delta t) = 0 \tag{3}$$

For the cyclic problem defined above, the stresses and strain rates will become asymptotic to a cyclic state where:

$$\sigma_{ij}(x_k,t) = \sigma_{ij}(x_k,t+\Delta t) \qquad \dot{\varepsilon}_{ij}(x_k,t) = \dot{\varepsilon}_{ij}(x_k,t+\Delta t) \tag{4}$$

It is worth noting that the above asymptotic cyclic solutions are common to all cyclic states associated with inelastic material behaviour including both the plasticity and creep.

2.2. Numerical procedure for the varying residual stress, creep strain and plastic strain range

Adopting the same minimum theorem for cyclic steady state solution and the same Linear Matching condition as described in [5, 6] for each iteration, we assume that plastic or creep strains occur at N instants, t_1, t_2.....t_N, where t_n corresponds to a sequence of points in the cyclic history. Hence the accumulation of inelastic strain over the cycle is $\Delta\varepsilon^T_{ij} = \sum_{n=1}^{N} \Delta\varepsilon_{ij}(t_n)$ where $\Delta\varepsilon_{ij}(t_n)$ is the increment of plastic or creep strain that occurs at time t_n. Define the shear modulus by linear matching

$$\sigma_0 = 2\bar{\mu}_n \bar{\varepsilon}(\Delta\varepsilon_{ij}(t_n)) \tag{5}$$

where σ_0 is the von Mises yield stress or creep flow stress and $\bar{\mu}_n$ is the iterative shear modulus. The von Mises yield stress σ_0 will be replaced by creep flow stress if the creep relaxation occurs at the load instance.

The Linear Matching Method procedure for the assessment of residual stress history and the

associated plastic or creep strain range due to the cyclic load history is described below. The entire iterative procedure includes a number of iteration cycles, where each cycle contains *N* iterations associated with *N* load instances. The first iteration is to evaluate the changing residual stress $\Delta\rho_{ij1}^{1}$ for the action of the elastic solution $\hat{\sigma}_{ij}^{e}(t_1)$ at the first load instance. We define $\Delta\rho_{ij_m}^{n}$ as the evaluated changing residual stress for *nth* load instance at *mth* cycle of iterations, where $n = 1, 2, ... N$ and $m = 1, 2, ... M$. At each iteration, the above changing residual stress $\Delta\rho_{ij_m}^{n}$ for *nth* load instance at *mth* cycle of iteration is calculated for the combined action of applied elastic stress at the *nth* load instance and previously calculated accumulation of residual stresses $\hat{\sigma}_{ij}^{e}(t_n)+\sum_{k=1}^{m-1}\sum_{l=1}^{N}\Delta\rho_{ij}{}_{k}^{l}+\sum_{l=1}^{n-1}\Delta\rho_{ij}{}_{m}^{l}$. When the convergence occurs at the *Mth* cycle of iterations, the summation of changing residual stresses at *N* time points must approach to zero ($\sum_{n=1}^{N}\Delta\rho_{ij_M}^{n}=0$) according to the condition of the steady state cyclic response. Hence the constant element of the residual stress for the cyclic loading history must be determined by

$$\bar{\rho}_{ij} = \sum_{n=1}^{N}\Delta\rho_{ij1}{}^{n} + \sum_{n=1}^{N}\Delta\rho_{ij2}{}^{n} + \cdots + \sum_{n=1}^{N}\Delta\rho_{ijM-1}{}^{n} \tag{6}$$

The corresponding increment of plastic strain occurring at time t_n is calculated by

$$\Delta\varepsilon_{ij}^{p}(t_n) = \frac{1}{2\bar{\mu}_n}\left[\hat{\sigma}_{ij}^{e}(t_n)' + \rho_{ij}(t_n)'\right] \tag{7}$$

where notation (') refers to the deviator component of $\hat{\sigma}_{ij}^{e}$ and ρ_{ij}. $\rho_{ij}(t_n)$ is the converged accumulated residual stress at the time instant t_n, i.e.

$$\rho_{ij}(t_n) = \bar{\rho}_{ij} + \sum_{k=1}^{n}\Delta\rho_{ijM}{}^{k} \tag{8}$$

In this paper, the Ramberg-Osgood type is adopted for the cyclic stress and strain range relationship:

$$\frac{\Delta\bar{\varepsilon}}{2} = \frac{\Delta\bar{\sigma}}{2E} + \left(\frac{\Delta\bar{\sigma}}{2B}\right)^{\frac{1}{\beta}} \tag{9}$$

where $\Delta\bar{\sigma}$ is the true stress range, $\Delta\bar{\varepsilon}$ is the true strain range, *E* is the elastic modulus, *B* and β are the Ramberg-Osgood plastic hardening constants. The first term on the right-hand side of the above equation represents the elastic strain amplitude and the second term corresponds to the plastic strain amplitude. Then the plastic strain range from Eq. (9) can be written as:

$$\Delta\bar{\varepsilon}_p = 2\left(\frac{\Delta\bar{\sigma}}{2B}\right)^{\frac{1}{\beta}} \tag{10}$$

If we define yield stress σ_0 in Eq. (5) as half stress range:

$$\sigma_0 = \frac{\Delta\bar{\sigma}}{2} = B\left(\frac{\Delta\bar{\varepsilon}_p}{2}\right)^{\beta} \tag{11}$$

then the iterative von-Mises yield stress $\sigma_0(t_n)$ from Ramberg-Osgood material model can be obtained from Eq. (7) as:

$$\sigma_0(t_n) = B\left(\frac{\bar{\varepsilon}(\Delta\varepsilon_{ij}^{p}(t_n))}{2}\right)^{\beta} \tag{12}$$

For the calculation of creep strain and stress relaxation during a creep dwell period, the relevant numerical scheme and theoretical formulations are summarized below.

2.3. Numerical procedure for the creep strain and flow stress

When calculating the creep strain during the dwell period, σ_0 in equation (5) equals to creep flow stress $\sigma_0 = \sigma_c$, which is an implicit function of creep strain $\Delta\varepsilon^c$ and residual stress $\Delta\rho^c$ during the creep dwell period.

Adopting a time hardening creep constitutive relation:

$$\dot{\bar{\varepsilon}}^c = B\bar{\sigma}^n t^m \tag{13}$$

where $\dot{\bar{\varepsilon}}^c$ is the effective creep strain rate, $\bar{\sigma}$ is the effective von Mises stress, *t* is the dwell time, and *B*, *m* and *n* are the creep constants of the material. When *m*=0, the time hardening constitutive equation becomes the Norton's law. During the relaxation process there exists an elastic follow up factor Z, i.e.

$$\dot{\bar{\varepsilon}}^c = -\frac{Z}{\bar{E}}\dot{\bar{\sigma}} \tag{14}$$

where $\bar{E} = 3E/2(1+\nu)$, *E* is the Young's modulus and $\dot{\bar{\sigma}} = \dot{\bar{\sigma}}(\sigma_{ij})$.

Combining (13) and (14) and integrating over the dwell time, we have

$$\frac{B\bar{E}\Delta t^{m+1}}{Z(m+1)} = \frac{1}{n-1}\left\{\frac{1}{(\bar{\sigma}_c)^{n-1}} - \frac{1}{(\bar{\sigma}_s)^{n-1}}\right\} \tag{15}$$

where $\bar{\sigma}_s$ is the effective value of the start of dwell stress, $\bar{\sigma}_c$ is the effective value of the creep flow stress at dwell time Δt, and $\bar{\sigma}_c = \bar{\sigma}(\sigma_{sij} + \Delta\rho_{cij})$. Integrating (14) gives the effective creep strain during the dwell period Δt as,

$$\Delta\bar{\varepsilon} = -\frac{Z}{\bar{E}}(\bar{\sigma}_c - \bar{\sigma}_s) \tag{16}$$

Combining (15) and (16) and eliminating $Z/\bar{E}$ gives

$$\Delta\bar{\varepsilon}^c = \frac{B(n-1)\Delta t^{m+1}(\bar{\sigma}_s - \bar{\sigma}_c)}{(\frac{1}{\bar{\sigma}_c^{n-1}} - \frac{1}{\bar{\sigma}_s^{n-1}})(m+1)} \tag{17}$$

For the pure creep where $\bar{\sigma}_s = \bar{\sigma}_c$, the creep strain becomes:

$$\Delta\bar{\varepsilon}^c = \frac{B\bar{\sigma}_s^n \Delta t^{m+1}}{m+1} \tag{18}$$

The creep strain rate $\dot{\bar{\varepsilon}}^F$ at the end of dwell time Δt is calculated by Eq. (15) and (17):

$$\dot{\bar{\varepsilon}}^F = B(\bar{\sigma}_c)^n \Delta t^m = \frac{\Delta\bar{\varepsilon}^c}{\Delta t}\frac{(m+1)}{(n-1)}\frac{\bar{\sigma}_c^n}{(\bar{\sigma}_s - \bar{\sigma}_c)}\left(\frac{1}{\bar{\sigma}_c^{n-1}} - \frac{1}{\bar{\sigma}_s^{n-1}}\right) \tag{19}$$

For the pure creep where $\bar{\sigma}_s = \bar{\sigma}_c$, the creep strain rate $\dot{\bar{\varepsilon}}^F$ becomes:

$$\dot{\bar{\varepsilon}}^F = B\left(\bar{\sigma}_s\right)^n \Delta t^m \tag{20}$$

Hence in the iterative process, we begin with current estimated $\bar{\sigma}_s^i$, $\bar{\sigma}_c^i$ and use Eq. (17), (19) or (20) to compute a new value of the creep stress $\bar{\sigma}_c$ from Eq. (21) to replace σ_0 in the linear matching condition (5):

$$\bar{\sigma}_c = \left(\frac{\bar{\dot{\varepsilon}}^F}{B\Delta t^m} \right)^{\frac{1}{n}} \tag{21}$$

To validate the efficiency and effectiveness of the numerical scheme, the proposed method was applied to benchmark examples of Bree problem and a holed plate [6]. In the next session of this paper, two types of weldments subjected to different reverse bending moments with various creep dwell periods are evaluated by the proposed method.

3. Numerical application: welded joints under high temperature–creep fatigue conditions

3.1. Problem Description

In this paper, the proposed LMM is applied to evaluate the creep fatigue lifetime of both Type 1 and Type 2 weldments [13] subjected to cyclic bending moment under creep condition. Fig. 2 shows the dimensions and configurations of the considered Type 1 and 2 welded joints, and the applied 2D symmetric FE model of the specimen assuming a plane strain condition with designation of different materials (parent, weld materials and heat-affected zone), boundary conditions and loading. A cyclic linear distribution of normal pressure P is applied to the end face of the parent material (Fig. 2) to simulate the reverse pure bending moment M, and a schematic bending moment loading history with a dwell period Δt considered for the creep-fatigue analysis is given in Fig.3. In addition to the pure fatigue case, one hour and 5 hours dwell periods are considered to investigate the effect of dwell period on the creep fatigue behavior. Five variants of reverse bending moment are analyzed, which correspond to 1.0%, 0.6%, 0.4%, 0.3% and 0.25% of total strain range at remote parent material.

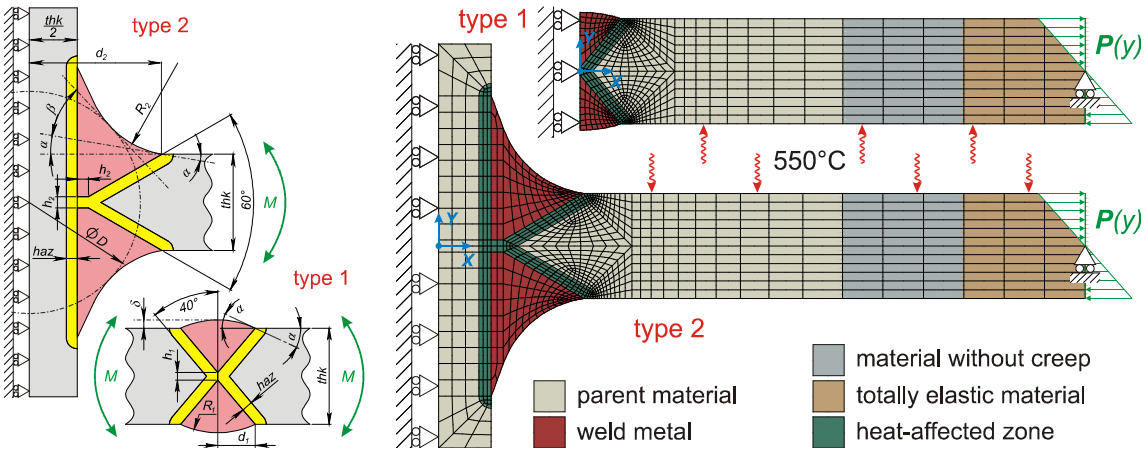

Figure 2. Dimensions and Finite Element models for Type 1 and Type 2 weldments, according to [13]

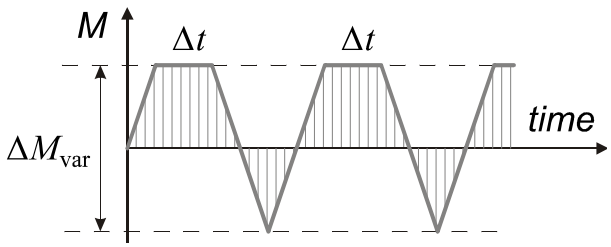

Figure 3. Schematic bending moment loading history for creep-fatigue analysis using the LMM

A Ramberg-Osgood formulation was adopted to simulate cyclic stress strain relationship, and a time hardening creep constitutive model was used to characterize creep behavior. The detailed material properties adopted are given in Table 1. In this creep fatigue damage assessment, the LMM was used to evaluate a steady-state cyclic behavior and to construct a saturated hysteresis loop. Then obtained total strain range during the cycle was used to assess fatigue damage combining R66 fatigue endurance curves [1]. The evaluated creep strain and stress relaxation data were adopted to evaluate creep damage considering time fraction rule and using the experimental creep rupture data. The final lifetime of the cruciform weldment was then obtained based on the calculated fatigue and creep damage under creep-fatigue interaction conditions.

Table 1. Material constants in Ramberg-Osgood model (Eq. 9) and creep time hardening model (Eq. 13)

Zone	E(MPa)	B(MPa)	β	σ_y(MPa)	A(MPa^{-n}/h)	n	m
Parent	160000	1741.96	0.2996	270.7	6.604e-19	5.769	-0.55
Weld	122000	578.99	0.1016	307.9	6.597e-23	7.596	-0.5
HAZ	154000	1632.31	0.2530	338.7	6.6e-21	6.683	-0.525

3.2. Numerical results and verifications

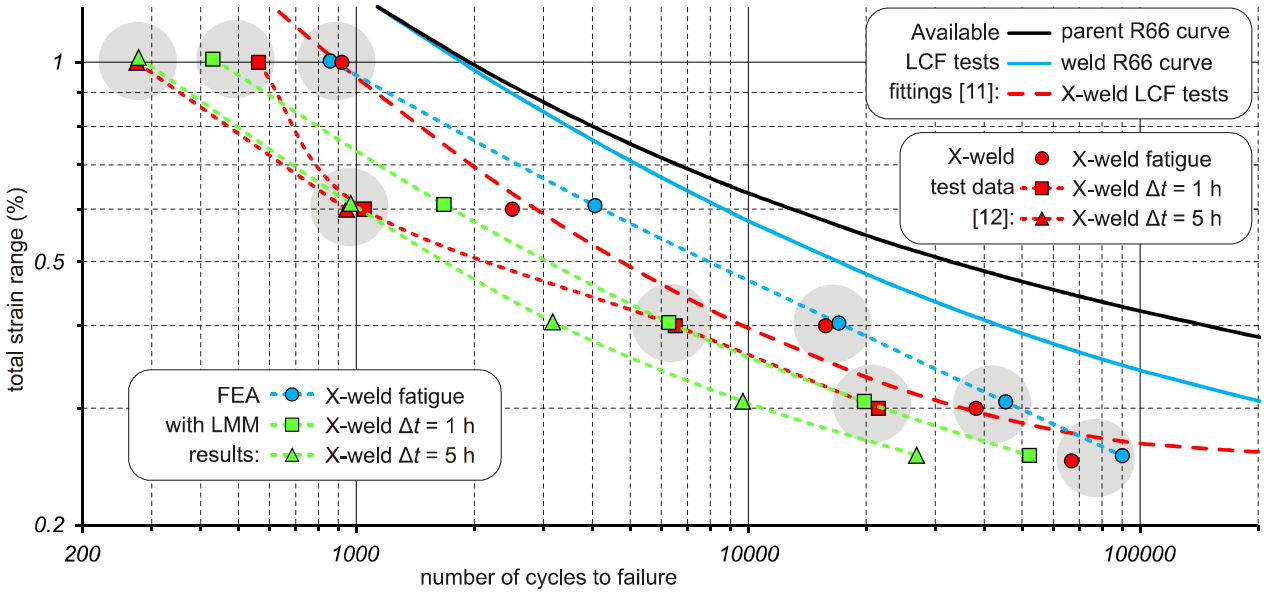

Figure 4. Results of creep-fatigue assessment in application to Type 2 cruciform weldment with experimental comparisons [11, 12]

The creep fatigue lifetime of Type 2 cruciform weldment assessed by the LMM and its experimental comparisons [11, 12] are presented in Fig. 4. Visual comparison of the observed and predicted number of cycles to failure in Fig. 4 for 3 variants of dwell period Δt (Δt=0 for pure fatigue) shows that 9 of the 11 simulations accurately predict the experimental results. Therefore, it can be used for the formulation of an analytic assessment model suitable for the fast estimation of lifetime for a variety of loading conditions. The low computational effort required by the LMM compared to other computational techniques makes it possible and relatively easy to extrapolate numerical predictions for loading conditions not captured by the available experiments.

The contour plots of LMM solutions including total strain range, creep strain, creep stresses at the beginning and end of dwell period, and the outputs of creep fatigue assessment procedure including

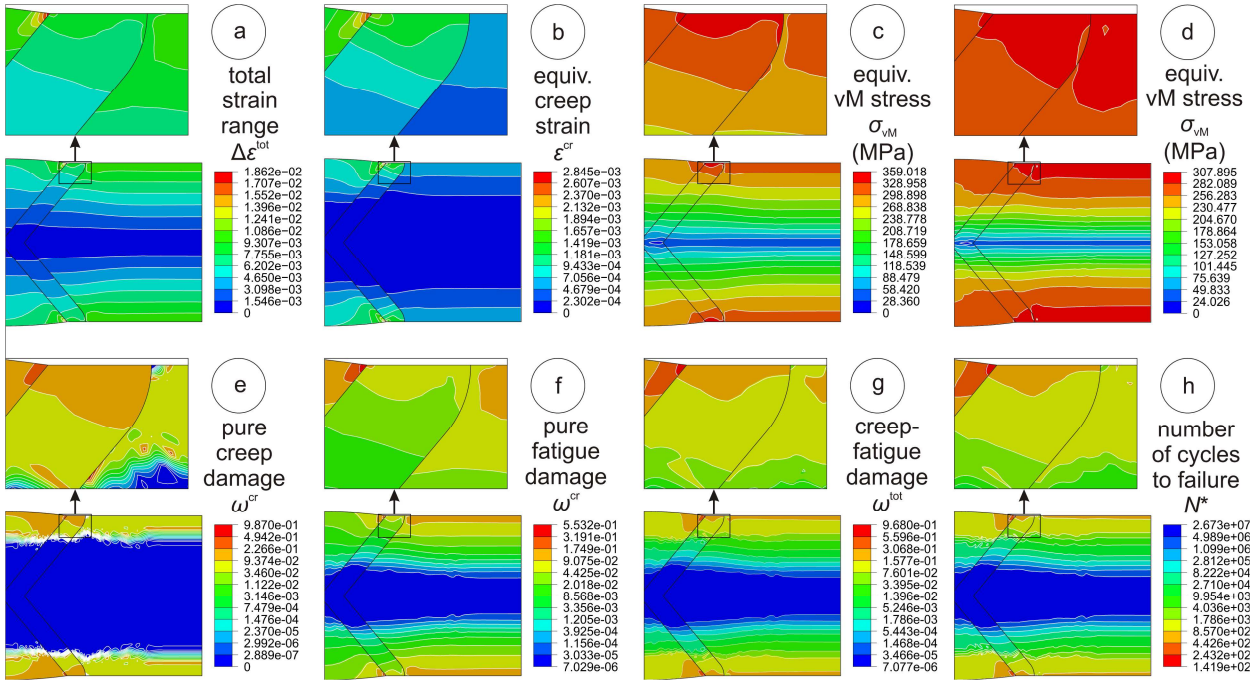

Figure 5. Contour plots of LMM results for type 1 weldment corresponding to $\Delta\varepsilon_{tot}$ = 1% on the outer fiber of plate and Δt = 5 hours of dwell period

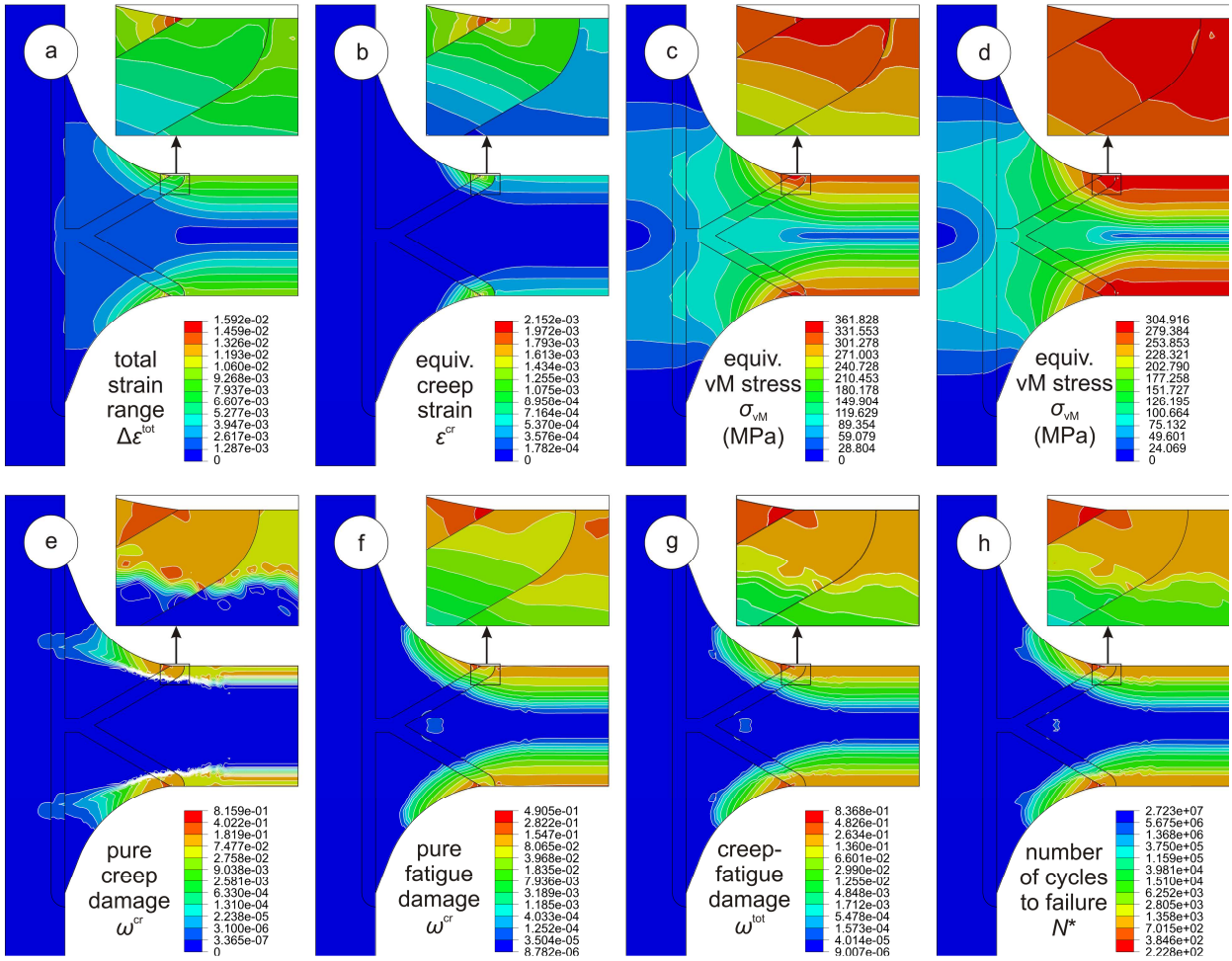

Figure 6. Contour plots of LMM results for type 2 weldment corresponding to $\Delta\varepsilon_{tot}$ = 1% on the outer fiber of plate and Δt = 5 hours of dwell period

pure creep damage, pure fatigue damage, creep-fatigue damage and number of cycles to failure are presented in Fig. 5 and 6 for Types 1 and 2 weldments corresponding to $\Delta\varepsilon_{tot}$ = 1% on the outer fiber of remote parent material and Δt = 5 hours of dwell period. It can be seen that both Types 1 and 2 weldments have the same critical location in the weld toe adjacent to HAZ. In terms of the accumulated total damage at failure, Type 1 weldment has less residual life (N* =142) than Type 2 weldment (N* =223) due to the increased values of parameters characterising hysteresis loop (e.g. total strain range and creep strain, see Figs. 5 and 6).

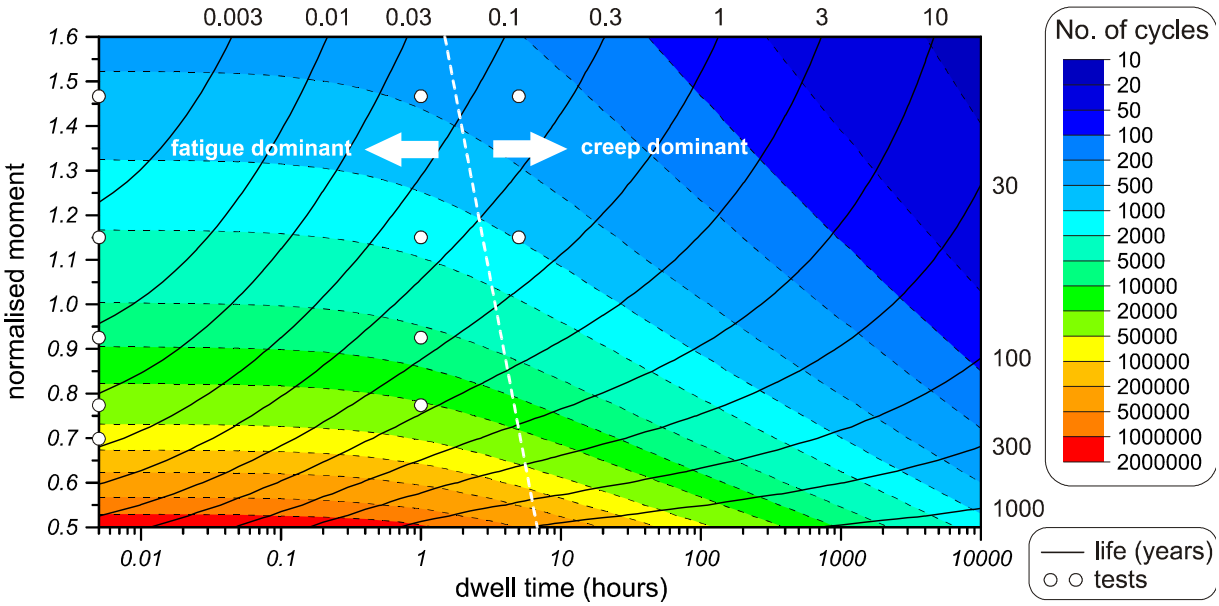

Figure 7. Design contour plot for creep-fatigue durability based on extrapolation of cycles to failure N^* and residual life L^*

The key engineering parameters including the numbers of cycle to failure N* and the residual life L* characterising creep-fatigue durability of the weldment have the principal importance for the design and assessment applications. For the purpose of usability, both parameters N* and L* obtained by LMM calculations and assessments can be represented in the form of design contour plot, shown in Fig. 7 for the Type 2 cruciform weldment. The contour lines (dashed for N* and solid for L*) allows a design engineer to define approximately and rapidly the level of reverse bending moment acceptable for the required service life and assumed average value of dwell period. For a given reverse bending moment and creep dwell period, the numbers of cycle to failure N* and the residual life L* of the cruciform weldment can be approximately estimated from Fig.7.

A full discussion of the solutions and further parametric studies are given by Gorash and Chen [14, 15], which demonstrate that, for such complex industrial problems, the LMM is capable of providing lifetime related solutions that are much more illuminating than conventional analysis.

4. Conclusions

This paper presents the latest development of the LMM on evaluation of the steady state behavior of an elastic plastic creep body subjected to cyclic loading under high temperature – creep fatigue conditions. The proposed LMM successfully calculates the plastic strain range, the creep stress and accumulated creep strain over a dwell period for a steady state load cycle by an iterative process using a general cyclic minimum theorem. Combining with the experimentally defined creep and fatigue damage data, the final lifetime of the component can then be obtained based on the

calculated fatigue and creep damage under creep-fatigue interaction conditions within the LMM framework.

By the application of the LMM to both Types 1 and 2 weldment subjected to reverse bending moment at creep fatigue condition with experimental comparisons, it confirms the efficiency and effectiveness of the proposed method for the creep fatigue damage assessment and demonstrates that LMM may be applied to complicated engineering applications with a much wider range of circumstances.

Acknowledgements

The authors deeply appreciate the Engineering and Physical Sciences Research Council (EPSRC) of the United Kingdom for the financial support (EP/G038880/1), the University of Strathclyde for hosting during the course of this work, and EDF Energy for the experimental data.

References

[1] R.A. Ainsworth, (Editor), R5: Assessment procedure for the high temperature response of structures, Issue 3, British Energy Generation Ltd, 2003.
[2] J. Bree, Elastic-plastic behaviour of thin tubes subjected to internal pressure and intermittent high-heat fluxes with application to fast-nuclear-reactor fuel elements. J strain anal, 2 (1967) 226–238.
[3] T. Nguyen, et al, Determination of the stabilized response of a structure undergoing cyclic thermal-mechanical loads by a direct cyclic method. ABAQUS Users' Conference Proceedings, 2003.
[4] ABAQUS, User's manual. Version 6.11, 2011.
[5] H.F. Chen, A.R.S. Ponter, Linear Matching Method on the evaluation of plastic and creep behaviours for bodies subjected to cyclic thermal and mechanical loading. International Journal for Numerical Methods in Engineering, 68 (2006) 13-32.
[6] H.F. Chen, W.H. Chen, J. Ure, A direct method on the evaluation of cyclic behavior with creep effect. ASME Pressure Vessels & Piping Division Conference, 2012.
[7] H.F. Chen, Lower and upper bound shakedown analysis of structures with temperature-dependent yield stress. Journal of Pressure Vessel Technology, 132 (2010) 1-8.
[8] H.F. Chen, A.R.S. Ponter, A direct method on the evaluation of ratchet limit, Journal of Pressure Vessel Technology, 132 (2010) 041202.
[9] H.F. Chen, M.J. Engelhardt, A.R.S. Ponter, Linear matching method for creep rupture assessment. International Journal of Pressure Vessels and Piping, 80 (2003) 213-220.
[10] D.J. Tipping, The Linear Matching Method: a guide to the ABAQUS user subroutines. E/REP/BBGB/0017/ GEN/07, British Energy Generation, 2007.
[11] S.K. Bate, J.P. Hayes, D.G. Hooton, N.G. Smith, Further analyses to validate the R5 volume 2/3 procedure for the assessment of austenitic weldments. SA/EIG/11890/R002, Serco Assurance, Warrington, UK, 2005.
[12] I. Bretherton, G. Knowles, J.P. Hayes, S.K. Bate, C.J. Austin, PC/AGR/5087: Final report on the fatigue and creep-fatigue behaviour of welded cruciform joints. RJCB/RD01186/R01, Serco Assurance, Warrington, UK, 2004.
[13] I. Bretherton, G. Knowles, I.J. Slater, S.F. Yellowlees, The fatigue and creep-fatigue behaviour of 26mm thick type 316L(N) welded cruciform joints at 550 C: An interim report. R/NE/432, AEA Technology plc, Warrington, UK, 1998.
[14] Y. Gorash, H.F. Chen, Creep fatigue life assessment of cruciform weldments using the linear matching method. Int J Press Vess Piping, (accepted) 2012.
[15] Y. Gorash, H.F. Chen, A parametric study on creep-fatigue strength of welded joints using the linear matching method. International Journal of Fatigue, (submitted) 2012.